*J. Fluid Mech.* (2009), *vol.* 625, *pp.* 125–133.  
doi:10.1017/S0022112009006089 Printed in the United Kingdom

# Estimating intermittency in three-dimensional Navier–Stokes turbulence

J. D. GIBBON†

Department of Mathematics, Imperial College London, London SW7 2AZ, UK

(Received 27 September 2008 and in revised form 9 January 2009)

The issue of why computational resolution in Navier–Stokes turbulence is hard to achieve is addressed. Under the assumption that the three-dimensional Navier–Stokes equations have a global attractor it is nevertheless shown that solutions can potentially behave differently in two distinct regions of space–time $\mathbb{S}^{\pm}$ where $\mathbb{S}^{-}$ is comprised of a union of disjoint space–time 'anomalies'. If $\mathbb{S}^{-}$ is non-empty it is dominated by large values of $|\nabla\boldsymbol{\omega}|$, which is consistent with the formation of vortex sheets or tightly coiled filaments. The local number of degrees of freedom $\mathcal{N}^{\pm}$ needed to resolve the regions in $\mathbb{S}^{\pm}$ satisfies $\mathcal{N}^{\pm}(\boldsymbol{x}, t) \lesssim 3\sqrt{2}\,\mathcal{R}_u^3$, where $\mathcal{R}_u = uL/\nu$ is a Reynolds number dependent on the local velocity field $u(\boldsymbol{x}, t)$.

## 1. Introduction

The space–time distribution and morphology of the vorticity and strain fields in three-dimensional Navier–Stokes turbulence has remained a puzzle, since Batchelor & Townsend (1949) discovered the phenomenon of intermittency in experimental flows. Instead of observing Gaussian behaviour in the flatness factor and similar quantities, they discovered the spiky spectra that are now recognized as typical for intermittent turbulent flows (see Kuo & Corrsin 1971; Douady, Couder & Brachet 1991; Meneveau & Sreenivasan 1991; Grossmann & Lohse 1993; Frisch 1995; Tsinober 2001; Zeff *et al.* 2003; Boffetta, Mazzino & Vulpiani 2008). The application of colour graphics in this past generation has dramatically illustrated how the morphologies of the vorticity and strain fields are typically dominated by 'thin sets' (see Yokokawa *et al.* 2002; Kurien & Taylor 2005). These sets usually form initially as quasi-two-dimensional vortex sheets which, under interaction, roll up into a tangle of quasi-one-dimensional tubes (Vincent & Meneguzzi 1994). It is also important to note that vorticity and strain accumulate on significantly different sets: indeed, there has been some debate over their relative importance (see Jimenez *et al.* 1993; Tsinober 1998, 2001). Figure 1, courtesy of Jörg Schumacher, is a snapshot illustration of the vorticity (enstrophy) field. Experiments show that these structures spontaneously appear and disappear as time evolves (Douady *et al.* 1991; Cadot, Douady & Couder 1995). While there exists an extensive literature on intermittency in the statistical physics literature concerning Kolmogorov's theory (Grossmann & Lohse 1993; Frisch 1995; Yakhot 2003; Boffetta *et al.* 2008), no satisfactory theoretical explanation for the high degree of space–time complexity of these phenomenon has ever been given based on three-dimensional Navier–Stokes solutions, nor has any mathematical explanation been forthcoming why vortex sheets should be, at least initially, the favoured topology. The consequences of this behaviour are far reaching. The spontaneous appearance of these structures, often at very short length scales, creates severe resolution problems

† E-mail address for correspondence: j.d.gibbon@ic.ac.uk

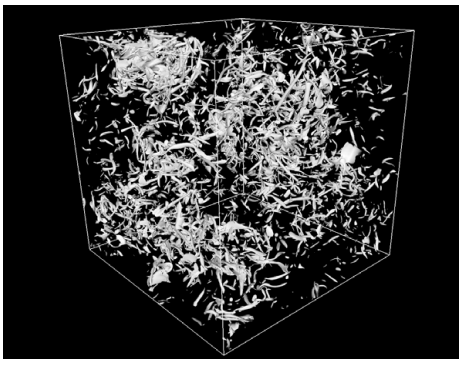

FIGURE 1. The figure, courtesy of Jörg Schumacher of the Technical University Ilmenau, is a three-dimensional statistically stationary homogeneous isotropic flow at a Taylor microscale Reynolds number of 107 showing iso-surfaces of $\omega^2$ at a level of 10 times the average of $\omega^2$. The cube with side-length $2\pi$ is resolved with $2048^3$ grid points which translates into 3-grid spacings for the Kolmogorov length $\Lambda_k$.

despite the increase of computing power in this past generation. To provide a partial theoretical explanation of this is one of the main aims of this paper. Landau's heuristic estimate for the number of degrees of freedom $\mathcal{N} \sim Re^{9/4}$ needed to resolve a turbulent flow is based on space–time averages and is by no means enough to resolve the thin structures discussed above (for instance, see Kerr 1985; Sreenivasan 2004; Schumacher, Sreenivasan & Yeung 2005; Schumacher, Sreenivasan & Yakhot 2007). An interesting result in this context is that of Yakhot (2003) who has applied rigorous methods to show that the inverse dissipation length scale associated with velocity structure functions has an upper bound proportional to $Re$ and not $Re^{3/4}$. Turning now to the status of Navier–Stokes solutions, there are generally two prevailing views. The first, which is an assumption generally held by the computational fluid dynamics community, is that the Navier–Stokes equations have regular solutions: that is, it is believed that unique solutions exist that can ultimately be resolved provided enough computing power is made available in the future. This is equivalent to the assumption that the Navier–Stokes equations possess strong solutions. The second view, held more by Navier–Stokes analysts, is that the unsolved regularity problem leaves open the possibility of singularity formation (Leray 1934; Ladyzhenskaya 1963; Constantin & Foias 1988; Foias *et al.* 2001). Caffarelli, Kohn & Nirenberg (1982) have shown that the potentially singular set has zero one-dimensional Hausdorff measure, which means that if singularities do occur in space–time then they must be rare events (see also Lin 1998; Ladyzhenskaya & Seregin 1999; Choe & Lewis 2000; Cheng 2004). For the purposes of providing a mathematical explanation for the resolution problem outlined above, the first assumption will be taken in this paper; that is, the Navier–Stokes equations are assumed to be regular. The nature of this assumption is discussed in § 3. It cannot be emphasized enough, however, that a flow may be regular but could nevertheless manifest highly intermittent events at fine scales, thus rendering the singular set empty.

## 2. Results based on space–time averages

The setting is the incompressible ($\mathrm{div}\,\boldsymbol{u} = 0$) three-dimensional Navier–Stokes equations for the velocity field $\boldsymbol{u}(\boldsymbol{x}, t)$ with mean-zero, divergence-free forcing $\boldsymbol{f}(\boldsymbol{x})$,

$$\boldsymbol{u}_t + \boldsymbol{u}\cdot\nabla\boldsymbol{u} = \nu\Delta\boldsymbol{u} - \nabla p + \boldsymbol{f}(\boldsymbol{x})\,, \tag{2.1}$$

on a periodic three-dimensional domain $\mathscr{V} = [0, L]^3$. Leray's energy inequality is derived by multiplying (2.1) by $\boldsymbol{u}$ and integrating over $\mathscr{V}$ to give

$$\frac{1}{2}\frac{\mathrm{d}}{\mathrm{d}t}\int_{\mathscr{V}} |\boldsymbol{u}|^2 \,\mathrm{d}V \leqslant -\nu \int_{\mathscr{V}} |\boldsymbol{\omega}|^2 \,\mathrm{d}V + \left(\int_{\mathscr{V}} |\boldsymbol{u}|^2 \,\mathrm{d}V\right)^{1/2} \left(\int_{\mathscr{V}} |\boldsymbol{f}|^2 \,\mathrm{d}V\right)^{1/2}, \tag{2.2}$$

where $\boldsymbol{\omega} = \operatorname{curl} \boldsymbol{u}$ is the vorticity. The method of Doering & Foias (2002) is now applicable in which the space–time averaged velocity $U$ and the energy dissipation rate $\varepsilon$

$$U^2 = L^{-3}\left\langle \int_{\mathscr{V}} |\boldsymbol{u}|^2 \,\mathrm{d}V \right\rangle, \quad \varepsilon = \nu L^{-3}\left\langle \int_{\mathscr{V}} |\boldsymbol{\omega}|^2 \,\mathrm{d}V \right\rangle \tag{2.3}$$

are found to be bounded quantities. In (2.3) the symbol $\langle \cdot \rangle$ for the long-time average is

$$\langle g \rangle = \limsup_{t\to\infty} \frac{1}{t}\int_0^t g(\tau)\,\mathrm{d}\tau\,. \tag{2.4}$$

For forcing concentrated around one length scale $\ell$ which, for simplicity, is taken to be $\ell = L/2\pi$, the Reynolds and Grashof numbers are defined by

$$Re = \frac{U\ell}{\nu}, \quad Gr = \frac{\ell^3 f_{r.m.s.}}{\nu^2}, \tag{2.5}$$

where $f_{r.m.s.}^2 = L^{-3}\int_{\mathscr{V}} |\boldsymbol{f}|^2 \,\mathrm{d}V$. From (2.2) we have

$$\left\langle \int_{\mathscr{V}} |\boldsymbol{\omega}|^2 \,\mathrm{d}V \right\rangle \leqslant \nu^2 L^{-1} Gr Re \qquad \Rightarrow \qquad \varepsilon \leqslant \nu^3 L^{-4} Gr Re\,. \tag{2.6}$$

Doering & Foias (2002) have shown that at high values of $Gr$ Navier–Stokes solutions obey $Gr \leqslant c\,Re^2$ and so the right-hand side of (2.6) can be estimated as $GrRe \leqslant c\,Re^3$. Estimates for the respective inverse Taylor microscale and Kolmogorov lengths are

$$\left(L\Lambda_T^{-1}\right)^2 = \frac{L^2\varepsilon}{\nu U^2} = \frac{\langle L^2 \int_{\mathscr{V}} |\boldsymbol{\omega}|^2 \,\mathrm{d}V\rangle}{\langle \int_{\mathscr{V}} |\boldsymbol{u}|^2 \,\mathrm{d}V\rangle} \leqslant c\,Re\,, \quad L\Lambda_k^{-1} = \left(\frac{\varepsilon}{\nu^3}\right)^{1/4} \leqslant c\,Re^{3/4}\,. \tag{2.7}$$

These upper bounds are consistent with Kolmogorov's scaling arguments (Frisch 1995). The Kolmogorov result leads to Landau's heuristic estimate for the number of degrees of freedom $\mathscr{N}(\Lambda_k) \leqslant c\,Re^{9/4}$ based on the number of vortices of volume $\Lambda_k^3$ relative to the volume $L^3$. These space–time averages have played a historically important role but they hide strong spiky variations in local behaviour. Two new results, extending (2.6) to higher moments of $\boldsymbol{\omega}$ ($m \geqslant 1$), are proved in the Appendix

$$\left\langle \left(\int_{\mathscr{V}} |\boldsymbol{\omega}|^{2m} \,\mathrm{d}V\right)^{1/(4m-3)} \right\rangle \leqslant c_{0,m}\nu^{2m/(4m-3)} L^{-1} Re^3 \tag{2.8}$$

and

$$\left\langle \left(\int_{\mathscr{V}} |\nabla\boldsymbol{\omega}|^{2m} \,\mathrm{d}V\right)^{1/(6m-3)} \right\rangle \leqslant c_{1,m}\nu^{2m/(6m-3)} L^{-1} Re^3\,. \tag{2.9}$$

These hint at some control over large fluctuations in $\boldsymbol{\omega}$ but not enough information is available to understand the behaviour of local space–time variations.

## 3. Local space–time results

The task is now to consider how a fluid can behave in local regions of space–time based on the assumption that solutions are regular. Some differences of definition are required, particularly in the Reynolds ($Re$) and Grashof ($Gr$) numbers of the last section, whose definitions were based on spatio-temporal and spatial averages, respectively. Local Reynolds and Grashof numbers are defined as

$$\mathscr{R}_u(\boldsymbol{x},\, t) = \frac{L|\boldsymbol{u}(\boldsymbol{x},t)|}{\nu}, \quad \mathscr{G}(\boldsymbol{x}) = \frac{L^3|\boldsymbol{f}(\boldsymbol{x})|}{\nu^2}\,. \tag{3.1}$$

We consider the evolution of the global enstrophy $\int_{\mathscr{V}} |\boldsymbol{\omega}|^2\,\mathrm{d}V$ using periodic boundary conditions and note that $\nabla\boldsymbol{\omega} \equiv \omega_{i,j}$ and $\operatorname{curl}\boldsymbol{\omega}$ are synonymous in $L^2$: that is $\int_{\mathscr{V}} |\nabla\boldsymbol{\omega}|^2\,\mathrm{d}V = \int_{\mathscr{V}} |\operatorname{curl}\boldsymbol{\omega}|^2\,\mathrm{d}V$. A rule for integration by parts can be deduced from the vector identity $\operatorname{div}(\boldsymbol{a}\times\boldsymbol{b}) = \boldsymbol{b}\cdot\operatorname{curl}\boldsymbol{a} - \boldsymbol{a}\cdot\operatorname{curl}\boldsymbol{b}$ under volume integration.

$$\begin{aligned}
\frac{1}{2}\frac{\mathrm{d}}{\mathrm{d}t}\int_{\mathscr{V}} |\boldsymbol{\omega}|^2\,\mathrm{d}V &= \int_{\mathscr{V}} \boldsymbol{\omega}\cdot\{\nu\Delta\boldsymbol{\omega} + \boldsymbol{\omega}\cdot\nabla\boldsymbol{u} + \operatorname{curl}\boldsymbol{f}\}\,\mathrm{d}V \\
&= \int_{\mathscr{V}} \{-\nu|\nabla\boldsymbol{\omega}|^2 - \boldsymbol{u}\cdot(\boldsymbol{\omega}\cdot\nabla)\boldsymbol{\omega} + \boldsymbol{f}\cdot\operatorname{curl}\boldsymbol{\omega}\}\,\mathrm{d}V \\
&\leqslant -\nu\int_{\mathscr{V}} |\nabla\boldsymbol{\omega}|^2\,\mathrm{d}V + \left(\int_{\mathscr{V}} |\boldsymbol{u}|^6\,\mathrm{d}V\right)^{1/6}\left(\int_{\mathscr{V}} |\boldsymbol{\omega}|^3\,\mathrm{d}V\right)^{1/3}\left(\int_{\mathscr{V}} |\nabla\boldsymbol{\omega}|^2\,\mathrm{d}V\right)^{1/2} \\
&\quad + \left(\int_{\mathscr{V}} |\nabla\boldsymbol{\omega}|^2\,\mathrm{d}V\right)^{1/2}\left(\int_{\mathscr{V}} |\boldsymbol{f}|^2\,\mathrm{d}V\right)^{1/2},
\end{aligned} \tag{3.2}$$

where the exponents 1/2, 1/6 and 1/3 in the Hölder inequality in the third line necessarily sum to unity. To estimate $\int_{\mathscr{V}} |\boldsymbol{\omega}|^3\,\mathrm{d}V$, we integrate by parts as indicated above and then use a vector identity and a Hölder inequality:

$$\begin{aligned}
\int_{\mathscr{V}} |\boldsymbol{\omega}|^3\,\mathrm{d}V &= \int_{\mathscr{V}} \boldsymbol{u}\cdot\operatorname{curl}(|\boldsymbol{\omega}|\boldsymbol{\omega})\,\mathrm{d}V \\
&\leqslant 2\left(\int_{\mathscr{V}} |\boldsymbol{u}|^6\,\mathrm{d}V\right)^{1/6}\left(\int_{\mathscr{V}} |\boldsymbol{\omega}|^3\,\mathrm{d}V\right)^{1/3}\left(\int_{\mathscr{V}} |\nabla\boldsymbol{\omega}|^3\,\mathrm{d}V\right)^{1/2},
\end{aligned} \tag{3.3}$$

whereupon we discover

$$\int_{\mathscr{V}} |\boldsymbol{\omega}|^3\,\mathrm{d}V \leqslant 3^{3/2}\left(\int_{\mathscr{V}} |\nabla\boldsymbol{\omega}|^2\,\mathrm{d}V\right)^{3/4}\left(\int_{\mathscr{V}} |\boldsymbol{u}|^6\,\mathrm{d}V\right)^{1/4}. \tag{3.4}$$

This allows us to re-write (3.2) as

$$\begin{aligned}
\frac{1}{2}\frac{\mathrm{d}}{\mathrm{d}t}\int_{\mathscr{V}} |\boldsymbol{\omega}|^2\,\mathrm{d}V \leqslant -\nu\int_{\mathscr{V}} |\nabla\boldsymbol{\omega}|^2\,\mathrm{d}V + \left(\nu\int_{\mathscr{V}} |\nabla\boldsymbol{\omega}|^2\,\mathrm{d}V\right)^{3/4}\left(9\nu^{-3}\int_{\mathscr{V}} |\boldsymbol{u}|^6\,\mathrm{d}V\right)^{1/4} \\
+ \left(\frac{1}{4}\nu\int_{\mathscr{V}} |\nabla\boldsymbol{\omega}|^2\,\mathrm{d}V\right)^{1/2}\left(4\nu^{-1}\int_{\mathscr{V}} |\boldsymbol{f}|^2\,\mathrm{d}V\right)^{1/2},
\end{aligned} \tag{3.5}$$

where factors of $\nu$ in the coefficients have been inserted appropriately. Two applications of the Hölder inequality $A^p B^q \leqslant pA + qB$ (with $p + q = 1$) finally give

$$\frac{1}{2}\frac{\mathrm{d}}{\mathrm{d}t}\int_{\mathscr{V}} |\boldsymbol{\omega}|^2 \,\mathrm{d}V \leqslant -\frac{\nu}{8}\int_{\mathscr{V}} |\nabla\boldsymbol{\omega}|^2 \,\mathrm{d}V + \frac{9}{4}\nu^{-3}\int_{\mathscr{V}} |\boldsymbol{u}|^6 \,\mathrm{d}V + 2\nu^{-1}\int_{\mathscr{V}} |\boldsymbol{f}|^2 \,\mathrm{d}V. \quad (3.6)$$

The appearance of the integral $\int_{\mathscr{V}} |\boldsymbol{u}|^6 \,\mathrm{d}V$ is a feature found by Cao & Titi (2007) in their study of the primitive equations for the ocean and atmosphere in which their regularity result revolved around a proof that the horizontal part of this integral is bounded. The degree of regularity that needs to be assumed for the Navier–Stokes equations is the existence of what is known as a global attractor (Constantin & Foias 1998; Foias *et al.* 2001), which means that $H_1(t) = \int_{\mathscr{V}} |\boldsymbol{\omega}(\cdot, t)|^2 \,\mathrm{d}V$ is assumed to be confined to a ball of finite radius in the limit $t \to \infty$. Thus, after multiplication by $L^6\nu^{-3}$, the integral of (3.6) over a time interval $[0, T]$ turns it into a space–time integral ($\omega_0 = L^{-2}\nu$)

$$\int_0^T \int_{\mathscr{V}} \left\{ -\frac{L^2}{8\omega_0^2}|\nabla\boldsymbol{\omega}|^2 + \frac{9}{4}\mathscr{R}_u^6 + 2\mathscr{G}^2 + \frac{H_1(0)}{2T\omega_0^3 L^3} \right\} \mathrm{d}V \,\mathrm{d}t > 0\,. \quad (3.7)$$

The right-hand side is positive because $H_1(T) > 0$ although there are no indications regarding its magnitude. Even though the four-integral in (3.7) is positive there may exist regions of space–time where the integrand is negative or zero. The consequences are

(*a*) There must be regions of space–time $\mathbb{S}^+ \subset \mathbb{R}^4$ where the integrand of the four-integral (3.7) is positive; that is

$$\frac{L^2}{8\omega_0^2}|\nabla\boldsymbol{\omega}|^2 < \frac{9}{4}\mathscr{R}_u^6 + 2\mathscr{G}^2 + O(T^{-1})\,. \quad (3.8)$$

(*b*) As noted above, there are potentially disjoint regions (anomalies) of space–time where the integrand of the four-integral (3.7) could be negative or zero, in which case

$$\frac{L^2}{8\omega_0^2}|\nabla\boldsymbol{\omega}|^2 \geqslant \frac{9}{4}\mathscr{R}_u^6 + 2\mathscr{G}^2 + O(T^{-1})\,. \quad (3.9)$$

If such regions exist we denote their union by $\mathbb{S}^- \subset \mathbb{R}^4$.

(*c*) It is usual to define the Kraichnan length based on the long-time averaged palenstrophy (see Foias *et al.* 2001 and Tsinober 2001). Its local equivalent is

$$\left(L\lambda_{kr}^{-1}\right)^6 = \frac{|\nabla\boldsymbol{\omega}|^2}{\nu^2} = \frac{L^2|\nabla\boldsymbol{\omega}|^2}{\omega_0^2}\,, \quad (3.10)$$

so (3.8) and (3.9) can be re-written as (ignoring the $T^{-1}$ terms for large $T$)

$$\begin{aligned} \left(L\lambda_{kr}^{-1}\right)^6 &< 18\,\mathscr{R}_u^6 + 16\mathscr{G}^2 \qquad \text{on} \qquad \mathbb{S}^+ \\ \left(L\lambda_{kr}^{-1}\right)^6 &\geqslant 8\,\mathscr{R}_u^6 + 16\mathscr{G}^2 \qquad \text{on} \qquad \mathbb{S}^-\,. \end{aligned} \quad (3.11)$$

Thus to resolve the structures in $\mathbb{S}^{\pm}$ the number of degrees of freedom is estimated as

$$\begin{aligned} \mathscr{N}^+ &< 3\sqrt{2}\,\mathscr{R}_u^3 + O(\mathscr{G}) \qquad \text{on} \qquad \mathbb{S}^+ \\ \mathscr{N}^- &\geqslant 2\sqrt{2}\,\mathscr{R}_u^3 + O(\mathscr{G}) \qquad \text{on} \qquad \mathbb{S}^- \end{aligned} \quad (3.12)$$

(*d*) Determining the shape and size of the sets $\mathbb{S}^{\pm}$ is an interesting question which cannot be answered until more regularity properties are established, nor does inequality (3.7) say anything about their statistics. The local palenstrophy $|\nabla\boldsymbol{\omega}|^2$ also has an independent constraint controlling its growth through (2.9). For the case $m = 1$, this can be written as

$$\left\langle \left( \int_{\mathscr{V}} |\nabla\boldsymbol{\omega}|^2 \, \mathrm{d}V \right)^{1/3} \right\rangle \leqslant c_{1,1} \nu^{2/3} L^{-1} Re^3 . \tag{3.13}$$

Because of the difference between the global and local Reynolds numbers $Re$ and $\mathscr{R}_u$, it is difficult to draw absolute conclusions based on (3.8), (3.9) and (3.13). Much depends upon how much $\mathscr{R}_u$ locally fluctuates about $Re$. Nevertheless, it is clear that the very large sixth-power local nonlinearity $\mathscr{R}_u^6$ acting as a lower bound in (3.9) amplifies the response in the magnitude of $|\nabla\boldsymbol{\omega}|^2$. It is possible that $\mathbb{S}^+$ and $\mathbb{S}^-$ may have similar sizes if the fluctuations in $\mathscr{R}_u$ are small or, alternatively, $\mathbb{S}^+$ may heavily dominate over $\mathbb{S}^-$ if the fluctuation is large. An example of the latter might occur if $\mathscr{R}_u > Re^{3/2}$ in subsets of $\mathbb{S}^-$. In this case, the lower bound in (3.9) is greater than the upper bound in (3.13), which is allowable only if this subset is sufficiently small and comparatively smaller values of $|\nabla\boldsymbol{\omega}|^2$ in $\mathbb{S}^+$ compensate for the larger than average values in $\mathbb{S}^-$. Thus, in a general sense, very large behaviour of $|\nabla\boldsymbol{\omega}|^2$ in $\mathbb{S}^-$ must therefore be balanced by smaller behaviour in $\mathbb{S}^+$. The result of this amplified and highly uneven response would be an intermittent spectrum. This is consistent with the remark of Batchelor & Townsend (1949) where they suggested that 'large wavenumber components are concentrated in isolated flow regions with an uneven energy distribution associated with the small-scale components'. Both they, and Emmons (1951), referred to this phenomenon as 'spottiness'.

Moreover, if a sudden increase of the gradient $|\nabla\boldsymbol{\omega}|$ occurs as one moves from a region in $\mathbb{S}^+$ across into an anomaly in $\mathbb{S}^-$ then this is consistent with the formation of vortex sheet-like structures or perhaps tightly coiled filaments (see Madja & Bertozzi 2001). The subsequent roll up of these sheets into tubes when they interact, as observed in numerical experiments (Vincent & Meneguzzi 1994), is not explained but the occurrence of both is consistent with the fact that both topologies have a small packing fraction.

## 4. Summary and discussion: vorticity versus strain

The arguments of the previous section show that even if solutions of the Navier–Stokes equations are assumed to live on a global attractor, space–time can potentially be split into two parts $\mathbb{S}^{\pm}$ with the potential for intermittent behaviour. Bounds on the number of degrees of freedom $\mathscr{N}^{\pm}$ in (3.12) are dependent on the velocity field at local space–time points of the flow. Particularly within $\mathbb{S}^-$, the value of $\mathscr{R}_u$ would have to be compared with $Re$: if $\mathscr{R}_u \gtrsim Re$ then the number of grid points needed to locally resolve that part of the flow would be significantly larger than the global average $Re^{9/4}$. This illustrates the need to monitor carefully values of $\mathscr{R}_u$ in a numerical calculation. The $L\lambda_k^{-1} > 18^{1/6}\mathscr{R}_u$ lower bound in $\mathbb{S}^-$ is similar in spirit to the result of Yakhot (2003) who concluded that the structure function inverse dissipation scale $\eta_{n,0}^{-1} = O(Re)$ is much larger than the inverse Kolmogorov scale $Re^{3/4}$. We agree with his conclusion that this places a severe constraint on the resolution requirements of direct numerical simulations of turbulence, and that existing simulations based on the

mesh-size $LRe^{-3/4}$ cannot accurately predict the properties of the violent structures of turbulence (Yakhot 2003).

These ideas can also be used in an alternative manner to see the effect of strain (see Jimenez *et al.* 1993; Tsinober 1998, 2000, 2001; Kerr 2001). It is more appropriate to define different local Reynolds numbers as

$$\mathscr{R}_\omega = \frac{L^2|\boldsymbol{\omega}|}{\nu}\,, \qquad \mathscr{R}_\rho = \frac{L^2\rho_s}{\nu}\,. \tag{4.1}$$

In (4.1) $\rho_s(\boldsymbol{x}, t)$ is the spectral radius of the strain rate matrix $\boldsymbol{S}$ which appears because $\boldsymbol{\omega}\cdot\boldsymbol{\omega}\cdot\nabla\boldsymbol{u} = \boldsymbol{\omega}\cdot\boldsymbol{S}\boldsymbol{\omega}$. The equivalent of the four-integral in (3.7) is

$$\int_0^T \int_{\mathscr{V}} \left\{ 2\mathscr{R}_\rho \mathscr{R}_\omega^2 - \frac{L^2}{\omega_0^2}|\nabla\boldsymbol{\omega}|^2 + \mathscr{G}^2 + O(T^{-1}) \right\} \mathrm{d}V\mathrm{d}t \geqslant 0\,. \tag{4.2}$$

Similar conclusions can be reached to those of § 3 regarding the effect the strain field and vorticity fields have on $|\nabla\boldsymbol{\omega}|$ in regions $\mathbb{S}_s^{\pm}$ of space–time. These will be different from those regions contained in $\mathbb{S}^{\pm}$ of (3.7). An estimate for the number of degrees of freedom needed to resolve $\mathbb{S}_s^{\pm}$ – the equivalent of (3.12) – is

$$\mathscr{N}_s^{\pm} \lesssim \sqrt{2}\,\mathscr{R}_\rho^{1/2}\mathscr{R}_\omega + O(\mathscr{G})\,. \tag{4.3}$$

My thanks to Panagiota Daskalopoulos, Charles Doering, Raymond Hide, Darryl Holm, Bob Kerr, Gerald Moore, Trevor Stuart, Edriss Titi, Jörg Schumacher and Arkady Tsinober for discussions. The referees made several helpful comments that have greatly improved the presentation of this paper.

## Appendix. Proof of (2.8) and (2.9) given in § 2

Consider the result of Foias, Guillopé & Temam (1981) for time averages of $H_n = \int_{\mathscr{V}} |\nabla^n\boldsymbol{u}|^2\mathrm{d}V$ which here are written in terms of $Gr$ and $Re$ ($n \geqslant 1$)

$$\left\langle H_n^{1/(2n-1)} \right\rangle \leqslant c_n \nu^{2/(2n-1)} L^{-1} GrRe\,. \tag{A 1}$$

Using the norm notation $\|\boldsymbol{\omega}\|_p^p = \int_{\mathscr{V}} |\boldsymbol{\omega}|^p \mathrm{d}V$, a Sobolev inequality gives

$$\|\boldsymbol{\omega}\|_{2m} \leqslant c_m \|\nabla^2\boldsymbol{\omega}\|_2^a \|\boldsymbol{\omega}\|_2^{1-a}, \tag{A 2}$$

where $a = 3(m-1)/4m$ for $m > 1$. Thus, taking $n = 3$ in (A 1), we have

$$\begin{aligned} \left\langle \|\boldsymbol{\omega}\|_{2m}^{2m/(4m-3)} \right\rangle &\leqslant c_{m,1} \left\langle \left(H_3^{1/5}\right)^{15(m-1)/4(4m-3)} H_1^{(m+3)/4(4m-3)} \right\rangle \\ &\leqslant c_{m,1} \left\langle \left(H_3^{1/5}\right) \right\rangle^{15(m-1)/4(4m-3)} \left\langle H_1 \right\rangle^{(m+3)/4(4m-3)} \\ &\leqslant c_{m,1} \nu^{2m/(4m-3)} L^{-1} GrRe\,. \end{aligned} \tag{A 3}$$

The result on $|\nabla\boldsymbol{\omega}|^{2m}$ in (2.9) can be found in the same way using $n = 4$ in (A 1).

## REFERENCES

Batchelor, G. K. & Townsend, A. A. 1949 The nature of turbulent flow at large wave-numbers. *Proc R. Soc. Lond.* A **199**, 238–255.

Boffetta, G., Mazzino, A. & Vulpiani, A. 2008 Twenty five years of multifractals in fully developed turbulence: a tribute to Giovanni Paladin. *J. Phys.* A **41**, 363001.

Cadot, O., Douady, S. & Couder, Y. 1995 Characterization of the low-pressure filaments in three-dimensional turbulent shear flow. *Phys. Fluids* **7**, 630–646.

Caffarelli, L., Kohn, R. & Nirenberg, L. 1982 Partial regularity of suitable weak solutions of the Navier-Stokes equations. *Comm. Pure Appl. Math.* **35**, 771–831.

Cao, C., & Titi, E. S. 2007 Global well-posedness of the three-dimensional viscous primitive equations of large scale ocean and atmosphere dynamics. *Ann. Math.* **166,** 245–267.

Cheng, H. 2004 On partial regularity for weak solutions to the Navier–Stokes equations. *J. Funct. Anal.* **211** (1), 153–162.

Choe, H. J. & Lewis, J. L. 2000 On the singular set in the Navier–Stokes equations. *J. Funct. Anal.* **175**, 348–369.

Constantin, P. & Foias, C. 1988 *Navier–Stokes Equations.* University of Chicago Press.

Doering, C. R. & Foias, C. 2002 Energy dissipation in body-forced turbulence. *J. Fluid Mech.* **467**, 289–306.

Douady, S., Couder, Y. & Brachet, M. E. 1991 Direct observation of the intermittency of intense vortex filaments in turbulence. *Phys. Rev. Letts.* **67**, 983–986.

Emmons, H. W. 1951 Laminar–turbulent transition in boundary layers. *J. Aero. Sci.* **18**, 490–498.

Foias, C., Guillopé, C. & Temam, R. 1981 New a priori estimates for Navier–Stokes equations in dimension 3. *Comm. Partial Diff. Eq.* **6**, 329–359.

Foias, C., Manley, O., Rosa, R. & Temam, R. 2001 *Navier–Stokes Equations & Turbulence.* Cambridge University Press.

Frisch, U. 1995 *Turbulence: The legacy of A. N. Kolmogorov.* Cambridge University Press.

Grossmann, S. & Lohse, D. 1993 Intermittency exponents. *Europhys. Lett.* **21**, 201–206.

Jimenez, J., Wray, A. A., Saffman, P. G. & Rogallo, R. S. 1993 The structure of intense vorticity in isopropic turbulence. *J. Fluid Mech.* **255**, 65–91.

Kerr, R. M. 1985 Higher order derivative correlations and the alignment of small–scale structures in isotropic numerical turbulence. *J. Fluid Mech.* **153**, 31–58.

Kerr, R. M. 2001 A new role for vorticity and singular dynamics in turbulence. In *Nonlinear Instability Analysis Volume II* (ed. L. Debnath), pp. 15–68. WIT Press.

Kuo, A. Y.-S. & Corrsin, S. 1971 Experiments on internal intermittency and fine-structure distribution functions in fully turbulent fluid. *J. Fluid Mech.* **50**, 285–320.

Kurien, S. & Taylor, M. 2005 Direct numerical simulation of turbulence: data generation and statistical analysis. *Los Alamos Sci.* **29**, 142–151.

Ladyzhenskaya, O. A. 1963 *The Mathematical Theory of Viscous Incompressible Flow.* Gordon and Breach.

Ladyzhenskaya, O. & Seregin, G. 1999 On partial regularity of suitable weak solutions of the three dimensional Navier–Stokes equations. *St. Petersburg Math. J.* **1**, 356–387.

Leray, J. 1934 Essai sur le mouvement d'un liquide visquex emplissant l'espace. *Acta Math.* **63**, 193–248.

Lin, F. 1998 A new proof of the Caffarelli, Kohn & Nirenberg theorem. *Comm. Pure Appl. Maths.* **51**, 241–257.

Madja, A. J. & Bertozzi, A. 2001 *Vorticity & Incompressible Flow.* Cambridge University Press.

Meneveau, C. & Sreenivasan, K. 1991 The multifractal nature of turbulent energy dissipation. *J. Fluid Mech.* **224**, 429–484.

Schumacher, J., Sreenivasan, K., & Yakhot, V. 2007 Asymptotic exponents from low-Reynolds-number flows. *New J. Phys.* **9**, 89–108.

Schumacher, J., Sreenivasan, K. R. & Yeung, P. K. 2005 Very fine structures in scalar mixing. *J. Fluid Mech.* **531**, 113–122.

Sreenivasan, K. R. 2004 Possible effects of small-scale intermittency in turbulent reacting flows. *Flow Turbul. Combust.* **72**, 115–141.

Tsinober, A. 1998 Is concentrated vorticity that important? *Eur. J. Mech B/Fluids* **17**, 421–449.

Tsinober, A. 2000 Vortex stretching versus production of strain/dissipation. In *Turbulence Structure & Vortex Dynamics* (ed. J. Hunt & J. Vassilicos), pp. 164–191. Cambridge University Press.

Tsinober, A. 2001 *An Informal Introduction to Turbulence.* Kluwer.

Vincent, A. & Meneguzzi, M. 1994 The dynamics of vorticity tubes of homogeneous turbulence. *J. Fluid Mech.* **225**, 245–254.

Yakhot, V. 2003 Pressure – velocity correlations and scaling exponents in turbulence. *J. Fluid Mech.* **495**, 135–143.

Yokokawa, M., Itakura, K., Uno, A., Ishihara, T. & Kaneda, Y. 2002 16.4-Tflops direct numerical simulation of turbulence by a Fourier spectral method on the Earth simulator. In *Proceedings of 2002 ACM/IEEE Conference on Supercomputing*, Baltimore pp. 1–17. IEEE Computer Society Press.

Zeff, B. W., Lanterman, D., McAllister, R., Roy, R., Kostelich, E. & Lathrop, D. 2003 Measuring intense rotation & dissipation in turbulent flows. *Nature* **421**, 146–149.